Universitat de les Illes Balears

FINAL DEGREE PROJECT

BALANCE BETWEEN ENTROPY AND PRECISION IN CHIRAL SYSTEMS

Irene Ribas Simal

Degree in Physics

Faculty of Sciences

Academic Year 2021-22

BALANCE BETWEEN ENTROPY AND PRECISION IN CHIRAL SYSTEMS

Irene Ribas Simal

FINAL DEGREE PROJECT

Faculty of Sciences

University of the Balearic Islands

Academic Year 2021-22

Key words:

Quantum, Topologycal, Chiral, Nanoestructures

Thesis Supervisor's Name Maria Rosa López Gonzalo

Tutor's Name (if applicable) Maria Rosa López Gonzalo

Abstract

This work focuses on the evaluation of the satisfaction of the Thermodynamic Uncertainty Relation that expresses a trade-off between dissipation and precision of a nonequilibrium current observable for a chiral system. It studies the case of a topological system with a quantum dot impurity acting under the influence of a Maxwell demon and how the influence of the demon can break the time-reversal symmetry of a Markov chain to avoid the lower bound of entropy production and current fluctuation for electrical currents

Contents

1. Introduction

Modern electronics are highly present in our everyday life and nanotechnology has an increasingly impactful role in them [1]. The search for faster and more powerful devices has led to the miniaturization of their components, allowing us to place an increasing amount of functionality in progressively reduced areas [2], [3]. Therefore, many advances regarding the manipulation of matter on an atomic scale have been made to develop the required nanostructures for the tasks. However, it is at such small dimensions that inter-atomic interactions and quantum effects, like the Quantum Hall effect [4] or the tunnel effect, are needed for describing the properties of the devices. In fact, these quantum effects are precisely those that cause novel behaviour that does not occur in larger magnitudes, which makes nanodevices more interesting.

The performance of these components is measured in terms of electrical currents. Thus, having a precise description and control over them is very useful. This is precisely the topic addressed in this study. There is a trade-off between precision and energy dissipation for nonequilibrium current observables called the Thermodynamic Uncertainty Relation (TUR) [5]–[8]. Originally derived for classical Markovian systems [9], this relation states that current fluctuations are lower bounded by the entropy production of the system. Therefore, having more precision for the current comes at the cost of producing more entropy and, consequently, dissipating more energy. This Final Degree Project aims to demonstrate that this TUR can be violated under certain circumstances of time irreversibility and electrostatic interaction asymmetry for a Markovian quantum system. More specifically, the proposed setup for this study will be a chiral system with a quantum dot impurity in a scenario that includes measurement and feedback.

The rest of this section introduces the basic notions about nanostructures and thermodynamics needed for the understanding of this work. Section 1.1 introduces the Thermodynamic Uncertainty Relation. Basic notions of confined systems are presented in Section 1.2 emphasizing the Quantum Dot and how Coulomb Interaction affects it. Then Section 1.3 introduces topological chiral systems and Section 1.4 explains what a Maxwell Demon is.

1.1. Thermodynamic Uncertainty Relation (TUR)

Fluctuations near equilibrium are completely characterized by the fluctuation-dissipation theorem of thermodynamics [10]. However, fluctuations present less universal structure when they are characterized far from equilibrium, leading to the problem of having to be handled on a case-by-case basis. Regarding this matter, Barato and Seifert [9] proposed a new kind of nonequilibrium principle, i.e., a thermodynamic uncertainty relation that expresses how the signal-to-noise ratio of a given observable is bounded by dissipation or entropy production as follows

$$\frac{\langle \delta\phi^2 \rangle}{\langle \phi \rangle^2} \geq \frac{2}{\langle \sigma \rangle} \tag{1}$$

Where $\langle \cdot \rangle$ denotes the ensemble average, $\langle \delta\phi^2 \rangle = \langle \phi^2 \rangle - \langle \phi \rangle^2$ is the variance, and σ is the entropy production. This definition considers stochastic processes that describe a sequence of events for which the probability of each event depends on the state of the previous event. In other words, the future of

the process depends only on the actual state, without any memory of what happened in the past. This stochastic model is called a Markov process or a Markov chain [11] and the TUR has been rigorously proven for current observables in time-homogeneous Markov dynamics with local detailed balance [5], [12], [13]. This work will study the validity of this TUR for a system with *broken* local detailed balance.

1.2. Confined Systems

Confined systems are defined as any system in which the motion of the charge carriers is restricted in one or more directions. These are categorized according to the number of dimensions of movement that are not constrained, from two to zero [14]. For example, the two-dimensional electron gas (2DEG) has its carriers moving freely in two spatial dimensions and constrained in the other, while quantum wires have carriers that travel freely only in one direction.

The definition of the charge distribution of confined systems begins with Schrödinger's time-independent equation, presented as

$$\left[\frac{\mathbf{p}^2}{2m} + V(\mathbf{r})\right]\psi = E\psi \qquad (2)$$

Where $\mathbf{p}$ is the particle momentum, m is its reduced mass, E is its energy and ψ is the wavefunction. If there is no confining potential $V(\mathbf{r}) = 0$, the free particle solution is obtained for equation (50). However, if there is, for example, a quantum potential well, the solutions are stationary states related to discrete energy levels. This means that the motion of particles can be restricted in a particular direction if a certain potential is applied.

1.2.1. From two to zero dimensions

The motion of electrons can be confined to two dimensions, called two-dimensional electron gas (2DEG), by forming a narrow interface between two different semiconductors with different *band gap* (e.g. GaAs and AlGaAs [15]). The separation between the conduction and valence bands acts as a confining potential restricting the electron motion from jumping between materials, as shown in the example of **Figure 3:**. Now, take **Figure 3:** as an example, the overlapping of thin layers of GaAs and AlAs results in finite quantum wells where electron motion is limited for the z-direction but free for the x,y-direction. These conditions give a solution to equation (50) as a separable wavefunction $\psi(x,y,z) = X_{k_x}(x)Y_{k_y}(y)Z_{n_z}(z) = \psi_{k_x,k_y,n_z}(x,y,z)$ that has plane wave expressions $(X_{k_x}, Y_{k_y}) = e^{i(k_x,k_y)(x,y)}$ for x,y-direction components and discrete stationary states for the z-direction component quantized by n_z. These electrons would have an energy $E_{n_z}(k_x,k_y) = \frac{\hbar^2 k_x^2}{2m*} + \frac{\hbar^2 k_y^2}{2m*} + E_{n_z}$ where the first two terms are the free particle energy with continuum values for momentums k_x and k_y and E_{n_z} are the discrete energy levels that confine the electron motion in the z-direction.

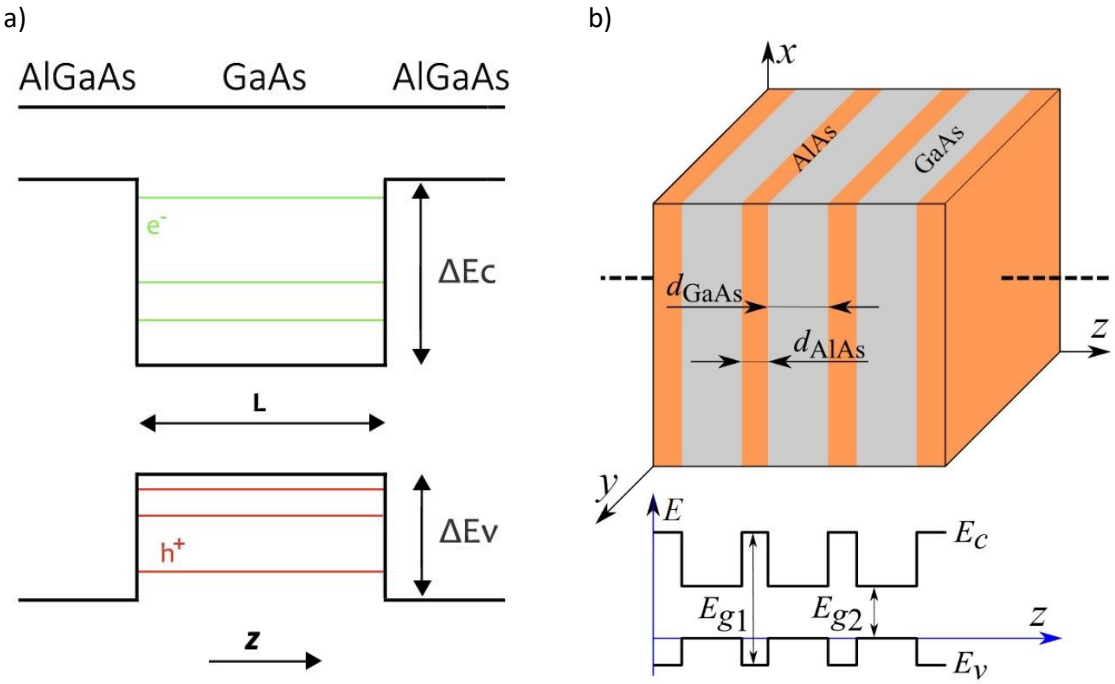

Figure 1: a) Schematic of a Type I AlGaAs/GaAs/AlGaAs quantum well [16]. Green lines represent electron energy levels, which are confined due to the difference in the conduction bands of the materials ΔEc. The same happens with the red lines that represent holes confined due to the difference in the valence bands of the materials ΔEv. b) GaAs/AlAs heterostructure arranged in a superlattice configuration [17].

Repeating this process for the other two directions would reduce the number of dimensions of the system. Starting with a 2DEG heterostructure, confinement in another direction, say the y-direction, would form a quantum wire, which corresponds to a one-dimensional system. Free electron motion is still possible along the axis of the wire, maintaining a continuum spectrum of one-dimensional states. Another way of building quantum wires could be using self-assembled structures from carbon nanotubes or epitaxially formed nanowires [18].

Finally, once the motion of the charge carriers is restricted in all three directions, zero-dimensional systems are obtained, giving rise to a completely discrete spectrum of bound states, similar to those of an isolated atom or molecule. These systems are called *quantum dots* or *artificial atoms* and are of special relevance for this work since they are the nanostructure studied for the TUR.

1.2.2. Quantum dots

Quantum dots are built by constricting the motion of electrons in all three dimensions and are nanostructures whose electronic states are completely quantized. There are many types of quantum dots depending on the fabrication method, for example: extending the lateral confinement of a wire structure to its remaining degree of freedom, cleaving a substrate of GaAs/AlGaAs during its MBE-growth [19], or growing such structures in the form of nano-pillars directly on a substrate in a process named self-assembly [20]. In any case, the zero-dimensional name is an idealization and quantum dots are modelled as 3-dimensional structures, like a sphere or a cube, with a radius of the order of nanometres so that from a macroscopic point of view, they look like dots. That is why they are usually referred to as quasi-zero-dimensional systems.

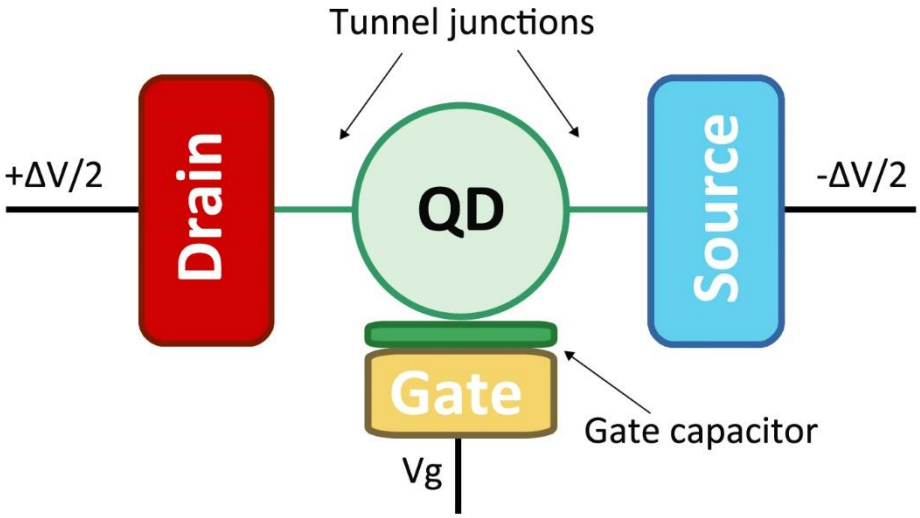

Figure 2: a) Sketch of a quantum dot transistor, where Vg is the potential applied to the gate that modifies the quantum dot's energy level and ΔV is the applied potential bias.

Among their many applications, their ability to store charge, acting similarly to a parallel plate capacitor is the most interesting for this study. A quantum dot can be capacitively coupled to an electrode, called the gate, with which the electronic potential of the dot can be controlled and, consequently, its active energy level ϵ_d. If the dot is coupled to reservoirs of electrons (**Figure 3:**) via tunneling barriers (using insulating materials), it is possible to make electrons flow through it one by one. That means that the dot only stores one electron at a time due to the electrostatic repulsion between charges, which produces the Coulomb Blockade. Because of this sequential transport, quantum dots can operate as Markov chains and as single electron transistors (SET).

1.2.3. Coulomb Interaction

The properties of quantum dots, similar to the properties of atoms, are modified by alterations in the number of electrons confined in the nanostructure. This happens due to what is called Coulomb Interaction [16] which has important effects at nanoscale magnitudes within temperatures slightly above zero Kelvin. Thus, the number of electrons is well defined if the quantum dot is practically isolated (using tunneling barriers), but it can still vary with single electron tunneling. How Coulomb Interaction affects the Quantum Dot system properties when adding an electron is explored below in more detail.

Consider the simple case in **Figure 3:** where a quantum dot is coupled to two reservoirs. This quantum dot has only one active level for the transport with energy ϵ_d because the rest of the levels are already occupied. The different electronic states that describe the system are $|0\rangle$ if the active dot level is empty and $|1\rangle$ if it has one electron. The electrochemical potentials of the left and right reservoirs are $\mu_L = E_F + eV_L$ and $\mu_R = E_F + eV_R$, respectively, where E_F is the Fermi Energy that they have in common and V_L, V_R are the externally applied voltages. Then, the electrochemical potential of the quantum dot determines the necessary energy for an electron to tunnel from a reservoir to the dot. Since there is electrostatic interaction, a charge Q inside the quantum dot would interact with an electron trying to get into it, which means that the energy level of the quantum dot is ϵ_d plus the interaction energy ΔU.

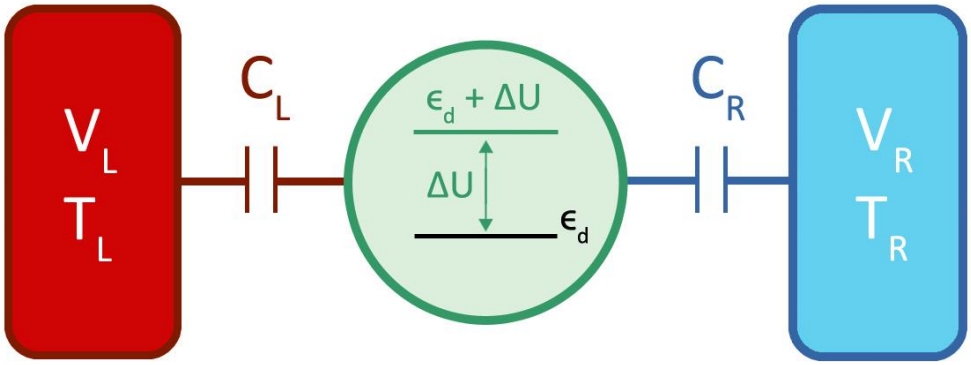

Figure 3: a) Schematic drawing of the Coulomb interaction in a quantum dot. Left (Right) reservoir has potential $V_{L(R)}$, temperature $T_{L(R)}$ and is capacitively coupled to the dot with capacitance $C_{L(R)}$. The energy level of the quantum dot is ϵ_d but is altered a quantity ΔU when an extra electron is inside.

The minimum charge that can be transferred to the dot is the elemental electron charge e, therefore Q can be assumed to be an integer number N of this electron charge $Q = Ne$. Hence, if the electrostatic energy of the dot without the extra electron is $U(Ne)$, and with the extra electron is $U\big((N+1)e\big)$ then the interaction energy carried by the electron is $\Delta U(Ne) = U\big((N+1)e\big) - U(Ne)$. Hence, the redefinition of the active level of the quantum dot is

$$\mu_d(Ne) = \epsilon_d + \Delta U(Ne) = \epsilon_d + U\big((N+1)e\big) - U(Ne) \qquad (3)$$

The electrochemical potential μ_d is the minimum energy required for introducing an electron to the dot, which means that the higher the potential, the more expensive it is to introduce an electron and, consequently, the more difficult it is for the transport to happen. Since the presence of an electron inside the dot (state $|1\rangle$) increases the energy level by a quantity ΔU due to the Coulomb Interaction, the energy of the electrons of the reservoirs L,R with $\mu_{L,R}$ is lower than the energy needed to enter the quantum dot μ_d and the quantum transport from the reservoirs to the dot is blocked until the electron inside the dot jumps out of it. This phenomenon is called the Coulomb Blockade and it is what produces the sequential transport of electrons.

Then, the energy level of the dot depends on the discrete number of charges N transferred to it. But since the quantum dot is coupled to two external sources at electric potentials V_L, V_R a polarization charge is created to keep the dot as a neutral charge object. Using a capacitive coupling model like the one shown in **Figure 3**, each coupling has an associated capacitance C_L, C_R that we can use to calculate the internal potential V_d of the quantum dot via the definition of the capacitance $C = Q/\Delta V$. For each reservoir coupling we have $C_i = Q_i/(V_d - V_i)$ so, if $Q = \sum_i Q_i$ and $C = C_R + C_L$ then the internal potential of the dot is

$$V_d = \frac{Q}{C} + \frac{C_L V_L + C_R V_R}{C} \qquad (4)$$

Using the definition of electrical potential $V = dU/dq$ and the assumption that $Q = Ne$ we obtain

$$U(Q) = \int_0^Q V_d(q)dq = \frac{Q^2}{2C} + \frac{C_L V_L + C_R V_R}{C} Q = \frac{(Ne)^2}{2C} + \frac{C_L V_L + C_R V_R}{C}(Ne) \qquad (5)$$

The first term is known as the charge energy $E_c = \frac{(Ne)^2}{2C}$, which will be commented on later. Then, applying equation (3), the electrochemical potential of the dot is defined as

$$\mu_d(N) = \epsilon_d + \frac{e^2}{2C} + \frac{Ne^2}{2C} + \frac{C_L V_L + C_R V_R}{C} e \qquad (6)$$

Because the dot has been defined with only two states: empty $|0\rangle$ or occupied $|1\rangle$, then $N = 0$ and $\Delta U(N \to N+1) = \Delta U(0 \to 1)$ obtaining

$$\mu_d = \left(\epsilon_d + \frac{e^2}{2C}\right) + \frac{C_L V_L + C_R V_R}{C} e = \tilde{\epsilon}_d + \frac{C_L V_L + C_R V_R}{C} e \qquad (7)$$

Where the level of the quantum dot has been redescribed as $\left(\epsilon_d + \frac{e^2}{2C}\right) \to \tilde{\epsilon}_d$ because the charge energy of the dot does not vary during the study.

However, Coulomb interactions are not guaranteed to be strong enough for Coulomb Blockade to occur, some requirements must be met. The charging energy $E_c = e^2/2C$, where C is the capacitance of the dot, is of relevance for the transport if it is greater than the thermal energy $k_B T$. In addition, the tunnel probability Γ must be low enough for the electrons to be well localized. In other words, the tunnel resistance R_t, which is inversely proportional to the tunnel probability Γ, must be strong enough for electrons to tunnel one by one. Since R_t defines the typical discharge time of a capacitor as $\Delta t = R_t C$, according to Heisenberg's uncertainty relation $\Delta t \Delta U = R_t C e^2/C > h$. This implies that the tunneling resistance is lower bound. To sum up, Coulomb Interaction will only be relevant if the following conditions are fulfilled [21]

$$R_t \gg \frac{h}{e^2}, \qquad \frac{e^2}{2C} \gg k_B \mathrm{T} \qquad (8)$$

These conditions can be achieved respectively by a weak coupling of the dot to the reservoirs and by making the dot small enough.

1.3. Topological Systems: Quantum Hall Effect [4]

A moving charge with velocity $\mathbf{v}$ influenced by a magnetic field $\mathbf{B}$ experiences a force $\mathbf{F} = \mathrm{q}\mathbf{v} \times \mathbf{B}$ perpendicular to the velocity and the magnetic field, diverting its trajectory. If $\mathbf{v}$ and $\mathbf{B}$ are perpendicular to each other, the trajectory becomes completely circular with a frequency $\omega = \frac{q|B|}{m}$ called the cyclotron frequency. This is what the Hall Effect is based on.

When a two-dimensional electron gas is subjected to a strong magnetic field, the electrons in the bulk describe cyclotron orbits with energy levels that are quantized and discrete (Landau levels). On the other hand, the electrons near the borders cannot complete the cyclotron orbits and instead make skipping orbits that follow the edges. This edge motion creates right and left chiral edge channels for transport since these electrons can move only in one direction "jumping" from one orbit to the next one as represented in **Figure 4a**. It is important to notice that changing the sign of the magnetic field would change the direction of the Lorentz force, causing the cyclotron and skipping orbits to change

their orientations, therefore changing the orientation of the edge states and modifying the chirality of the system.

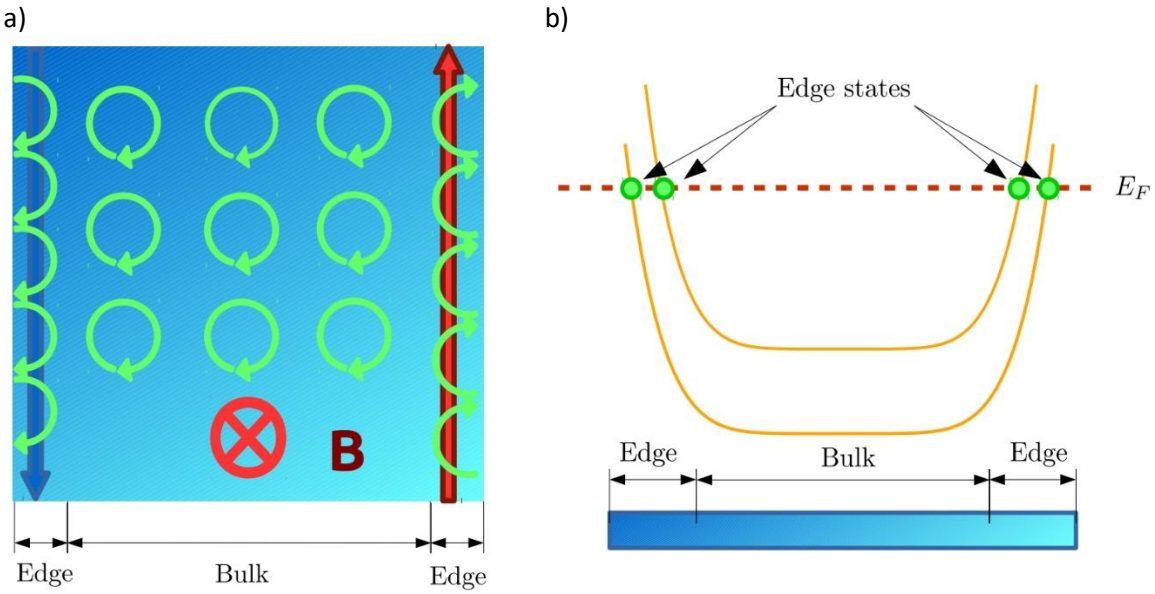

Figure 4: Quantum Hall Effect a) Represents the cyclotron orbits of the charges in a 2DEG subjected to a strong magnetic field B. b) Representation of the Landau levels (Yellow) and how they are flat in the bulk but rise near the edges, crossing the Fermi Energy and creating the Edge states. Reprinted from [21].

For a deeper perspective of the *Quantum Hall Effect*, it is important to mention that the Landau levels for electrons under the influence of a magnetic field have a degeneracy of $\frac{S}{2\pi}\frac{eB}{\hbar}$ with S being the area of the plane they can move in. If the magnetic field $\mathbf{B}$ is especially strong, the degeneracy of the Landau levels describing the cyclotronic orbits of the electrons of the bulk is extremely big, which allows all the electrons to be in just a few Landau levels. Therefore, the conduction band is essentially flat in the bulk and the corresponding Landau energies are practically constant as represented in **Figure 4b**. However, in the zones close to the boundaries that confine the electrons, the conduction band rises above the Fermi level and each occupied Landau level in the interior of the 2DEG intersects the Fermi level at two points located at opposite ends of the sample. Consequently, this yields two propagating edge states with different directions that function as current channels. This process serves to produce systems where charge flows alongside their borders but act as insulators on the bulk, also referred to as *topological systems*.

1.4. Maxwell Demon

Maxwell proposed in his *gedankenexperiment* [22] (or mental experiment) the idea of an entity capable of separating warm and cold particles of gas without performing work, apparently violating the second law of thermodynamics. How this ideal entity, the Maxwell Demon, works, is explained below.

The second law of thermodynamics can be expressed in many specific ways, but one simple statement of it is that, unless energy is supplied, heat always moves from a hotter system to a colder one. Another version of the law establishes the concept of entropy S as a physical property of a thermodynamic system, stating that the universal entropy cannot decrease $\Delta S_{Universe} \geq 0$ for any isolated system left to spontaneous evolution. This means that isolated systems always reach thermodynamic equilibrium where the entropy is highest at the given internal energy. If a process is irreversible, then $\Delta S_{Universe} > 0$ which implies that dissipation occurs. For a heat engine, this means that not all heat can be converted to work and vice versa since a part of it is dissipated through the irreversibility of the process.

Statistical mechanics gave a new definition of the entropy $S = K_B \ln(\Omega)$ where Ω is the number of microstates (states that define all possible microscopic variables). Therefore, entropy can be interpreted as a degree of disorder or "microscopic chaos" and, dissipation, as the work or energy needed to disorder the system. To the Statistical Mechanics description, there is a higher probability of finding a system in a macroscopic configuration that maximizes the number of possible microscopic states, in other words, a more disordered one. But this law does not forbid the system to be in any other macroscopic configuration, for it is not a physical law, but a statistical one that states that a system evolves from a lesser probable state to a more probable one. Here is where the Maxwell Demon intervenes.

In his *gedankenexperiment*, Maxwell considered the following: There is a gas inside an isolated container divided into two portions, *A* and *B,* by a wall with a hole. It is a known fact that gas molecules inside a vessel at uniform temperature are moving with velocities by no means uniform, even though the mean velocity of any great number of them is almost exactly uniform. Then, imagine an ideal entity capable of distinguishing individual molecules. If this being opens and closes the hole, allowing only the faster molecules to pass from B to A and the slower ones to pass from A to B, he would, without any expenditure of work, raise the temperature of A and lower the temperature of B, in contradiction to the second law of thermodynamics.

This apparent paradox was sorted using Claude Shannon's information theory, where information is treated as a physical magnitude that obeys physical laws. A system with more entropy has more possible microstates and, consequently, needs more information to be characterized. Therefore, the entropy of a system is directly connected to the information it contains.

By identifying the state of the particles, the demon is making a measure and acquiring information from it. This information needs to be stored, but because the demon cannot infinitely store it, information must be erased. Erasing information implies energy dissipation that compensates for the entropy reduction the system undergoes because of the demon's intervention, solving the paradox and satisfying the second law of thermodynamics.

This work implements a protocol that mimics Maxwell's demon idea but to transport charge currents against a set potential difference.

2. The Setup

The proposed system for evaluating the TUR is exposed in this section and it is represented in Figure 5. The system consists of a topological system in the presence of a magnetic field $\mathbf{B}$, as explained before in section **¡Error! No se encuentra el origen de la referencia.**, with a quantum dot inside acting as an i mpurity. The system is connected to two electron reservoirs L and R, each one with its own electrochemical potential $\mu_{L,R} = E_F + eV_{L,R}$ and temperature T_L, T_R. Because topological systems are insulators in their bulk, the electrons provided by the reservoirs can only travel through the channels created by the edges (i.e., through the edge states). Therefore, each edge state is associated with the electrochemical potential of a reservoir. Since the chirality of the system depends on the sign of the magnetic field (justified in section **¡Error! No se encuentra el origen de la referencia.**) the direction of t hese edge states also depends on it. This means that which reservoir's electrochemical potential is associated with the edge state varies according to the sign of the magnetic field.

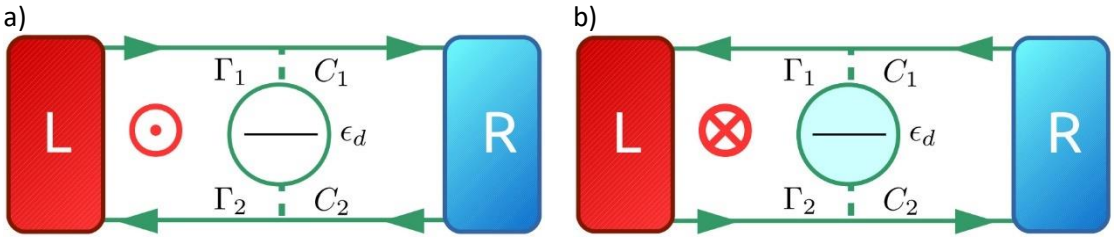

Figure 5: The diagram represents the dispositive with a quantum dot impurity of energy level ϵ_d and the edge states are represented by green arrows 1, 2 connected to the reservoirs L, R. The electrons from the edge states interact with the dot through the tunnel probabilities Γ_1 and Γ_2 and the capacitances C_1 and C_2. In a) there is $\mathbf{B} > 0$, so the upper (lower) edge state travels as $L \rightarrow R$ ($R \rightarrow L$), while in b) there is $\mathbf{B} < 0$, so the upper (lower) edge state travels as $R \rightarrow L$ ($L \rightarrow R$). Reprinted from [21]

Electrons on the edge states can jump to the empty level of the quantum dot with tunneling probabilities Γ_1 and Γ_2 following a model of capacitances C_1 and C_2 where the subscript refers to the upper and lower edge states, respectively.

Following the model that was presented in section 1.2.3, the energy of the quantum dot is given by equation (7), but the situation is a little bit different. The dot is not coupled directly to the reservoirs, but to the edge states instead, therefore $\{C_L, C_R, V_L, V_R\} \rightarrow \{C_1, C_2, V_1, V_2\}$. However, the potential of the edge states takes the value of the potential of a reservoir depending on the sign of the magnetic field. Then, there are two possible energies of the quantum dot obtained using equation (7):

- μ_d^+ where $+$ denotes the positive sign of the magnetic field $\mathbf{B} > 0$ and has $V_{1,2}^+ \equiv V_{L,R}$

$$\mu_d^+ = \tilde{\epsilon}_d + \frac{C_1 V_L + C_2 V_R}{C} e = \tilde{\epsilon}_d + \frac{(\eta + 1)}{2} eV_L - \frac{(\eta - 1)}{2} eV_R \qquad (9)$$

- μ_d^- where $-$ denotes the negative sign of the magnetic field $\mathbf{B} < 0$ and has $V_{1,2}^+ \equiv V_{L,R}$

$$\mu_d^- = \tilde{\epsilon}_d + \frac{C_1 V_R + C_2 V_L}{C} e = \tilde{\epsilon}_d + \frac{(\eta+1)}{2} eV_R - \frac{(\eta-1)}{2} eV_L \quad (10)$$

A new parameter $\eta = \frac{C_1 - C_2}{C_1 + C_2}$, $\eta \in \{-1,1\}$ that defines the asymmetry between capacitances has been introduced for the above equations. Notice that the difference between both energy levels becomes

$$\mu_d^+ - \mu_d^- = e\eta(V_L - V_R) \quad (11)$$

This shows that there is a discrepancy between the energy levels of both magnetic field configurations only when the setup has a potential bias applied ($V_R \neq V_L$) and when capacitances are asymmetric $\eta \neq 1$. These are the parameters that will be controlled and modified for the tests carried out in this study. Equation (11) also reveals that changing the sign of η is equivalent to changing the sign of $\Delta V = V_L - V_R$, providing equal values of $\mu_d^+ - \mu_d^-$.

2.1. Maxwell Demon protocol

As it was mentioned above, a shift in the sign of the magnetic field causes a change in the chirality of the edge states, breaking the time-reversal symmetry. Consequently, the local detailed balance is also broken due to the electronic interactions in the quantum dot. This situation provides the possibility to create a protocol that mimics the behaviour of the Maxwell Demon and to investigate the consequences of applying it to the setup, verifying if it can violate the TUR. This demon will change the sign of the magnetic field depending on the absence $\mathbf{B} > 0$ or presence $\mathbf{B} < 0$ of an extra electron inside the dot.

Taking $\eta < 0$ and $\Delta V = V_L - V_R > 0$ values for which $\mu_d^- > \mu_d^+$, the protocol is represented in **Figure 2** performing the following steps [21]:

Step 1: Starting with $\mathbf{B} > 0$ and the dot empty. The process begins when an electron coming from the right reservoir enters the dot through the lower edge state. The tunneling probability for this event was Γ_2, the model capacitance C_2 and the energy of the electron in the dot is μ_d^+.

Step 2: The demon detects an electron inside the dot and changes the magnetic field to $\mathbf{B} < 0$. This raises the energy level for the localized state of the dot to μ_d^-.

Step 3: Because $\mu_d^- > \mu_d^+$ it is easier for the electron inside the dot to transition to the left reservoir through the upper edge state with Γ_1 and C_1. Accomplishing a charge transport from R to L, against the voltage bias ΔV. ($V_L > V_R$)

Step 4: The demon detects the absence of the electron inside the quantum dot and reverses the magnetic field again to $\mathbf{B} > 0$, returning to step 1. In this step, the demon erases the collected information, dissipating energy and increasing the entropy.

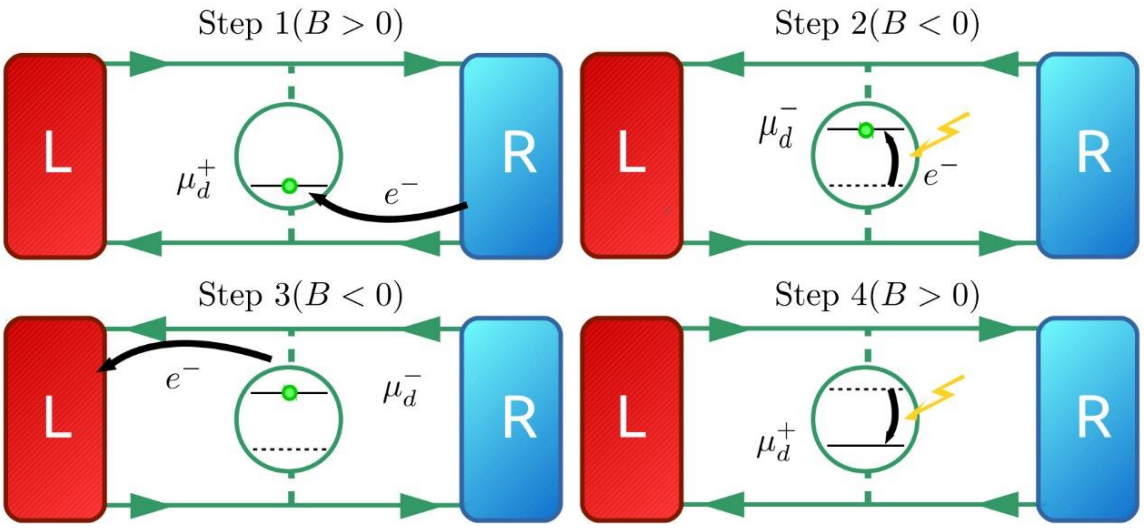

Figure 6: Visual representation of the demon protocol steps for pushing electrons against a voltage bias. The yellow lightning represents the demon's actions. Reprinted from [21]

This protocol requires two conditions to be met for the demon to be able to transform information into energy:

- The electrostatic interactions must be asymmetric when the magnetic field is switched by the demon → $|\eta| > 0$
- Tunneling events between the edge states and the localized quantum dot states must be energy-dependent.

3. Theoretical Model

In the previous section, we defined the setup as a topological system containing a quantum dot coupled to two reservoirs with a macroscopic number of electrons. Since the system is weakly coupled to the reservoirs, the transport occurs sequentially and the charge states of the system are well defined. Therefore, only two states are considered for the dot with an energy level μ_d: one where the dot is empty $|0\rangle$ and the other, where the dot is occupied $|1\rangle$. Then, the system can be fully characterized using these charge states, and transitions between them happen as electrons transfer. These transitions occur with certain probabilities $W_{f\leftarrow i}$ called transition rates, where the "i" index denotes the state of the system before the transition, and the "f" index denotes the state towards which the system is transitioning. Thus, the probability P_m to find the system in a state $|m\rangle$ using the Master Equation [23] can be obtained.

$$\frac{\partial P_m}{\partial t} = \sum_{m' \neq m} W_{mm'} P_{m'} - W_{m'm} P_m \qquad (12)$$

Where $\mathrm{m}, m' = \{0,1\}$ are the different charge states of the dot. The master equation then defines the time-dependent variation of P_m as the difference between the probability of transitioning from any other state $|m'\rangle$ to the state $|m\rangle$ and the probability of transitioning from the state $|m\rangle$ to any other

state $|m'\rangle$. Because our quantum dot is coupled to two reservoirs, the electron can jump into or out of the left (L) or right (R) reservoir. Consequently, both contributions to the transition rates $v = \{L, R\}$ must be considered.

$$W_{mm'} = \sum_{v} W^{v}_{mm'} \tag{13}$$

Combining (12) and (13), the following expression is obtained:

$$\frac{\partial P_m}{\partial t} = \sum_{m' \neq m, v} W^{v}_{mm'} P_{m'} - W^{v}_{m'm} P_m \tag{14}$$

And then, the explicit expressions for the proposed system can be written as

$$\frac{\partial P_0}{\partial t} = (W^{L}_{01} + W^{R}_{01}) P_1 - (W^{L}_{10} + W^{R}_{10}) P_0 \tag{15}$$

$$\frac{\partial P_1}{\partial t} = (W^{L}_{10} + W^{R}_{10}) P_0 - (W^{L}_{01} + W^{R}_{01}) P_1 \tag{16}$$

From equations (15) and (16), it can be observed that $\dot{P}_0 = -\dot{P}_1$ which must be satisfied for the state probabilities of a system with only two states. However, because the parameters defining the system do not vary in time, neither do the rates that define the transitions. Then, the stationary solution to the equations can be obtained by considering that $\dot{P}_0 = \dot{P}_1 = 0$, which also implies that the sum of the probabilities must be unity: $P_0 + P_1 = 1$. This can also be interpreted as particle conservation since the number of electrons entering the quantum dot equals the number of electrons leaving it. Thus, the equation system is solved to obtain

$$P_0 = \frac{W^{L}_{01} + W^{R}_{01}}{W^{L}_{01} + W^{R}_{01} + W^{L}_{10} + W^{R}_{10}} \tag{17}$$

$$P_1 = \frac{W^{L}_{10} + W^{R}_{10}}{W^{L}_{01} + W^{R}_{01} + W^{L}_{10} + W^{R}_{10}} \tag{18}$$

This result is expected as the probability of finding the system in the state $|0\rangle$ ($|1\rangle$) is the sum of both contributions L and R of the transition rates to the state $|0\rangle$ ($|1\rangle$) normalized to the sum of all the transition probabilities.

3.1. Quantum transport properties

Once the proposed system is characterized using the Master Equation, the next step is to obtain the necessary analytical expressions required to evaluate the Thermodynamic Uncertainty Relation. The assumed criterion is as follows: any current (charge, heat, entropy…) that enters the reservoirs is considered positive and any current that leaves them, is negative.

3.1.1. Charge current

Following said sign criterion, the charge current I_v is defined as the net charge that flows into the reservoir v. This current can be obtained simply by "counting" the electrons so that the net flow is the difference between the electrons flowing into the reservoir and the electrons flowing out of it.

$$I_v = e(W_{01}^v P_1 - W_{10}^v P_0) \quad (19)$$

Substituting here equations (17) and (18) and rearranging, the following expressions are obtained for the charge currents that flow into the R and L reservoirs

$$I_L = e\frac{W_{01}^L W_{10}^R - W_{10}^L W_{01}^R}{W_{01}^L + W_{01}^R + W_{10}^L + W_{10}^R} \quad (20)$$

$$I_R = e\frac{W_{10}^L W_{01}^R - W_{01}^L W_{10}^R}{W_{01}^L + W_{01}^R + W_{10}^L + W_{10}^R} \quad (21)$$

Notice that $I_L + I_R = 0$ due to the sequential nature of the transport through the quantum dot since no charge can be stored in it.

3.1.2. Energy and heat currents

Using the same procedure, the net energy flowing into the reservoirs can be obtained by counting the number of electrons flowing into and out of them and the energy they are carrying, μ_d. On the other hand, since heat is transferred energy, the amount of energy each electron transfers to the reservoir v from the dot is $\mu_d - \mu_v$. Respectively, the expressions for the heat and energy currents to the reservoir v depending on the sign of the magnetic field are

$$J_v = (\mu_d - \mu_v)W_{01}^v P_1 - (\mu_d - \mu_v)W_{10}^v P_0 \quad (22)$$

$$J_v^E = \mu_d W_{01}^v P_1 - \mu_d W_{10}^v P_0 \quad (23)$$

It can be confirmed that the sum of these heat currents verifies the Joule effect of energy dissipation $\sum_v J_v = -I\Delta V$. However, since the Maxwell protocol is applied to this system (See sec. 2.1. Maxwell Demon protocol), the energy that electrons carry is μ_d^+ when they flow from the reservoirs to the quantum dot $0 \to 1$ and μ_d^- when they flow from the dot to the reservoirs $1 \to 0$ and equations (22) and (23) turn into

$$J_v = (\mu_d^- - \mu_v)W_{01}^v P_1 - (\mu_d^+ - \mu_v)W_{10}^v P_0 \quad (24)$$

$$J_v^E = \mu_d^- W_{01}^v P_1 - \mu_d^+ W_{10}^v P_0 \quad (25)$$

Apparently, these expressions no longer verify the Joule effect, but that is because a part of the energy is dissipated by the demon. Since charge only flows between the system and the reservoirs the energy that the demon receives is purely in the form of heat. In section 1.4. Maxwell Demon it was explained that the demon paradox is resolved using information theory, which means that there is a part of the

heat (24) that is used for erasing the information the demon collects. Then, by energy conservation $J_L^E + J_R^E + J_D = 0$ and using equations (11), (17) and (18), the energy current that flows to the demon can be obtained as

$$J_D = \mu_d^+(W_{10}^L + W_{10}^R)P_0 - \mu_d^-(W_{01}^L + W_{01}^R)P_1 = e\eta\Delta V \frac{(W_{10}^L + W_{10}^R)(W_{01}^L + W_{01}^R)}{W_{01}^L + W_{01}^R + W_{10}^L + W_{10}^R} \quad (26)$$

This result implies that the energy flow to the demon depends on the voltage bias applied and the capacitance asymmetry.

3.1.3. Entropy production

As it was mentioned before, the ideal Maxwell demon extracts information from the system in order to perform. This means that the entropy production has a component resulting from the information current that flows into the demon and cannot be calculated using the heat currents as Clausius entropy would do. Then, using Shannon's entropy expression [24] $S(t) = -k_B \sum_m P_m(t) \ln P_m(t)$, its time derivative can be obtained as

$$\dot{S}(t) = -k_B \sum_m \dot{P}_m(t) [\ln P_m(t) + 1] = -k_B \sum_m \dot{P}_m(t) \ln P_m(t) \quad (27)$$

Where $\dot{P}_m(t) = dP_m/dt$ and $\sum_m \dot{P}_m(t) = d\sum_m dP_m/dt = 0$ due to probability conservation. Using the master equation (12) and omitting for compactness of notation the dependence of S and P_m on t, the following equation is obtained

$$\dot{S} = -k_B \sum_{m,n} [W_{mm'}P_{m'} - W_{m'm}P_m] \ln P_m \quad (28)$$

Since m and m' are dummy variables and transition rates $W_{f\leftarrow i}$ have a component for each reservoir v, as expressed in equation (13)**¡Error! No se encuentra el origen de la referencia.**, the equation above can be rewritten in the form

$$\dot{S} = -k_B \sum_{v,m,n} W_{mm'}^v P_{m'} \ln \frac{P_m}{P_{m'}} \quad (29)$$

Now, the entropy balance $\dot{S} = \dot{S}_e + \dot{S}_i$ is divided into an entropy flow $\dot{S}_e$ and an entropy production $\dot{S}_i$ that satisfy $\dot{S}_i = -\dot{S}_e$ for the stationary case since $\dot{S} = 0$. These two quantities have the expressions (30) and (31) [21], [23].

$$\dot{S}_i = k_B \sum_{mm'v} W_{mm'}^v P_{m'} \ln\left(\frac{W_{mm'}^v P_{m'}}{W_{m'm}^v P_m}\right) \quad (30)$$

$$\dot{S}_e = -k_B \sum_{mm'v} W_{mm'}^v P_{m'} \ln\left(\frac{W_{mm'}^v}{W_{m'm}^v}\right) \quad (31)$$

Using (31), the expressions for the charge currents (20) and (21), the fact that $I_L = -I_R$, and that $\dot{S}_i = -\dot{S}_e$, the entropy production for the proposed system acquires the following explicit form

$$\dot{S}_i = -\dot{S}_e = \frac{I_L}{e} k_B \ln\left(\frac{W_{01}^L W_{10}^R}{W_{10}^L W_{01}^R}\right) \quad (32)$$

Later we will show that $\dot{S}_i$ depends on the intensity of the charge current but not on its sign.

3.1.4. Charge current noise

The current noise generated in the proposed system can be obtained by introducing counting fields, which are "information mechanisms" that count the charges that travel through the dot. This approach uses Full Counting Statistics adapting the Master Equation (12) into the Quantum Master Equation [25], which depends on the density matrix ρ, in order to add the counting fields to the characterization of the system. Then, the Fourier transformation of the Quantum Master Equation is

$$\frac{d}{dt}\rho(\chi, t) = -\mathcal{L}(\chi)\rho(\chi, t) \quad (33)$$

Where $\mathcal{L}$ is the Liouville *superoperator* used to describe the time evolution of a reduced density matrix describing a Markovian system in interaction with a bath, or, in this case, with the system edge estates. The value of χ is arbitrary and t is the time variable. For the proposed system, the Liouvillian $\mathcal{L}$ is [26]

$$\mathcal{L}(\chi) = \begin{pmatrix} W_{01}^R + W_{01}^L & -W_{10}^L e^{i\chi} + W_{10}^R \\ -W_{01}^L e^{-i\chi} + W_{01}^R & W_{10}^R + W_{10}^L \end{pmatrix} \quad (34)$$

Then, the Cumulant Generating Function for the charge current is derived using Flindt's method [27], which uses the Rayleigh-Schrödinger perturbation theory. In Flindt's method, the following operators are defined

$$\tilde{\mathcal{L}}(\chi) = \mathcal{L}(\chi) - \mathcal{L} = \begin{pmatrix} 0 & -W_{10}^L e^{i\chi} + W_{10}^L \\ -W_{01}^L e^{-i\chi} + W_{01}^L & 0 \end{pmatrix} \quad (35)$$

$$\mathcal{P} = |\alpha\rangle\langle\tilde{\alpha}|, \qquad \mathcal{Q} = 1 - \mathcal{P}, \qquad \mathcal{R} = \mathcal{Q}\,\mathcal{L}^{-1}\mathcal{Q} \quad (36)$$

Here, $\mathcal{L} = \mathcal{L}(0)$, the $\mathcal{L}^{-1}$ stands for the Drazin inverse of $\mathcal{L}$, and the ket vectors are defined as

$$|\alpha\rangle = \begin{pmatrix} P_0 \\ P_1 \end{pmatrix}, \qquad |\tilde{\alpha}\rangle = \begin{pmatrix} 1 \\ 1 \end{pmatrix} \quad (37)$$

Then, the second cumulant can be obtained by solving the equation

$$C_2 = \left[\langle\tilde{\alpha}|\tilde{\mathcal{L}}^{(2)}|\alpha\rangle - 2\langle\tilde{\alpha}|\tilde{\mathcal{L}}^{(1)}\mathcal{R}\tilde{\mathcal{L}}^{(1)}|\alpha\rangle\right] \quad (38)$$

where

$$\tilde{\mathcal{L}}^{(n)} = \partial_{i\chi}^n \tilde{\mathcal{L}}(\chi)\big|_{\chi=0} \quad (39)$$

And the explicit expressions for the derivatives are obtained as

$$\tilde{\mathcal{L}}^{(1)} = \begin{pmatrix} 0 & -W_{10}^{L} \\ W_{01}^{L} & 0 \end{pmatrix}, \qquad \tilde{\mathcal{L}}^{(2)} = \begin{pmatrix} 0 & -W_{10}^{L} \\ -W_{01}^{L} & 0 \end{pmatrix} \tag{40}$$

Carrying out the corresponding matrix and ket operations of equation (38), the second cumulant can be obtained and, hence, the noise of the charge current flowing through the quantum dot $\mathrm{C}_2 \equiv \langle \delta I^2 \rangle$.

3.2. Transition rates

Once all the expressions for the TUR's thermodynamic variables have been obtained, there's still one more step to fully characterize the system: calculating the *transition rates* (or *tunneling rates* since all electron transfer events are tunneling events) as functions of the gate and bias voltages. These rates are defined as the average number of transitions happening between the states $|i\rangle$ and $|f\rangle$.

Since here the transitions occur between a continuum of states in the v reservoir and the discrete state of the dot, Fermi's Golden rule can be applied to calculate the transition rates as follows

$$W_{f \leftarrow i} = \int_{-\infty}^{\infty} \Gamma_{fi}(E)\, \rho_i(E - \mu_i) \bar{\rho}_f\big(E - \mu_f\big) dE \tag{41}$$

In this notation, Γ_{fi} represents the tunneling probability through the edge states while $\rho_i(E)$ and $\bar{\rho}_f(E)$ represent respectively the electron and hole density of the states. Then, equation (41) can be understood as the probability of transitioning from an initial state $|i\rangle$ towards a final state $|f\rangle$ multiplied by the average number of states $|i\rangle$ that can tunnel and by the average number of states $|f\rangle$ that can "accept" the tunneling, just like holes that can accept electrons.

If the electron and hole density represent a state of the dot, they are equal to a Dirac delta function $\rho_i(E) = \bar{\rho}_i(E) = \delta(E)$. On the contrary, considering that electrons are fermions and should follow the Fermi-Dirac statistics, the electron density of the states of the reservoir v has a Fermi-Dirac distribution $\rho_i(E) = f_v(E)$ with the hole density being the opposite $\bar{\rho}_i(E) = 1 - f_v(E)$. This $f_v(E)$ is the Fermi function (42).

$$f_v(E) = \frac{1}{1 + e^{\frac{E}{k_B T_v}}} \tag{42}$$

Here, T_v is the temperature of the v reservoir and k_B is Boltzmann's constant.

3.2.1. Transition rates for the Maxwell Demon Protocol

In this study, tunneling probabilities are assumed to be constant $\Gamma_\alpha(E) = \Gamma_\alpha$ and equal for both edge states $\Gamma_1 = \Gamma_2 = \Gamma$. Also, considering that these transitions happen between the quantum dot and two different reservoirs (L or R) with different properties and that there cannot be more than one electron inside the dot, the only possible transitions in the proposed system are

$$W_{1 \leftarrow 0}^{L,R} = \Gamma \int_{-\infty}^{\infty} f_{L,R}\big(E - \mu_{L,R}\big) \delta(E - \mu_d) dE \tag{43}$$

$$W_{0\leftarrow 1}^{L,R} = \Gamma \int_{-\infty}^{\infty} \left[1 - f_{L,R}\left(E - \mu_{L,R}\right)\right] \delta(E - \mu_d) dE \quad (44)$$

Solving equations (43) and (44), the following expressions are obtained

$$W_{10}^{L,R} = \Gamma f_{L,R}\left(\mu_d^{\pm} - \mu_{L,R}\right) \quad (45)$$

$$W_{01}^{L,R} = \Gamma \left[1 - f_{L,R}\left(\mu_d^{\pm} - \mu_{L,R}\right)\right] \quad (46)$$

As was previously mentioned, the demon modifies the sign of the magnetic field depending on the absence $(B > 0)$ or presence $(B < 0)$ of an electron inside the quantum dot. This means that the transition rates of electrons leaving the dot $W_{01}^{L,R}$ have the level of the quantum dot being μ_d^- while the transition rates of electrons entering the dot $W_{10}^{L,R}$ have the level of the quantum dot being μ_d^+. If we consider that the Fermi Energy used to describe de electrochemical potential of the reservoirs has zero value for this study, it does not influence the transport properties of the system. Therefore, the electrochemical potentials will be defined as $\mu_{L,R} = eV_{L,R}$ for the rest of the sections obtaining the following results

$$W_{10}^{L,R} = \Gamma f_{L,R}\left(\mu_d^{+} - eV_{L,R}\right) \qquad B > 0 \quad (47)$$

$$W_{01}^{L,R} = \Gamma \left[1 - f_{L,R}\left(\mu_d^{-} - eV_{L,R}\right)\right] \qquad B < 0 \quad (48)$$

Now, all the variables required for characterizing the state of the proposed system have been defined and formal results can be obtained.

4. Results

The results displayed in this section are obtained following the theoretical model presented in section 3 for the system proposed in section 2. The and using the Maxwell demon protocol. The focus here will be to obtain the variations of the different properties of the quantum transport under different values of the voltage bias ΔV and the quantum dot modified energy level (which will be represented as $\epsilon_d = \tilde{\epsilon}_d$ for simplicity) in order to evaluate the satisfaction of the Thermodynamic Uncertainty Relation presented in section 1.1. Thermodynamic Uncertainty Relation (TUR) .

For the sake of clarity, the system of units taken has that $h = e = 1$ and takes a reference tunneling probability Γ = 1 where the rest of the magnitudes will be expressed as a function of Γ. In this context, because Γ is a magnitude of time: the electrical current will be measured in units of $\frac{e\Gamma}{h}$, the heat current in units of $\frac{\Gamma^2}{h}$, the entropy flow in $\frac{k_B\Gamma}{h}$, the temperature in $\frac{\Gamma}{k_B}$, the voltage bias in $\frac{\Gamma}{e}$, the noise in units of $\frac{e^2\Gamma}{h}$ and energy in the units of Γ.

4.1. Charge currents

We start calculating the charge current of the system. As was mentioned in section 3.1.1. Charge current, due to the sequential nature of the transport, the charge that enters the dot must leave the

dot, which means that $I_L + I_R = 0$. Thus, we consider that the current that flows through the systems is $< I >= I_L$. In this framework, when the current flows from the right reservoir to the left reservoir ($R \to L$), the current flow is considered positive $I_L > 0$ and when the current flows from the left reservoir to the right reservoir ($L \to R$), the current flow is negative $I_L < 0$.

Using equation (20) we notice that the sign (direction) of the charge flow depends on the sign of $W_{01}^{L} W_{10}^{R} - W_{10}^{L} W_{01}^{R}$. The quotient between these transition rates, calculated using (47) and (48), is

$$Qu = \frac{W_{01}^{L} W_{10}^{R}}{W_{10}^{L} W_{01}^{R}} = \frac{[1 - f_L(\mu_d^- - eV_L)]\, f_R(\mu_d^+ - eV_R)}{[1 - f_R(\mu_d^- - eV_R)]\, f_L(\mu_d^+ - eV_L)} \qquad (49)$$

Here $\pm$ denotes the sign of the magnetic field. Notice that equation (49) gives $Qu = 1$ when there is no current, $Qu < 1$ when the current is negative and $Qu > 1$ when the current is positive. If there is a temperature gradient $\Delta T = T_L - T_R$ but not a potential bias $\Delta V = 0$ then we obtain a weak current depending on ΔT because of the Seebeck effect [28] but it is unaltered by the application of a magnetic field due to the electrochemical potentials for both orientations being equal $\mu_d = \mu_d^- = \mu_d^+$. Consequently, charge currents generated by the thermoelectric effect are unaltered by the demon and temperature gradients will not be considered. Removing the temperature bias so that $T_0 = T_R = T_L$, when there is no potential bias applied, the quotient has a value of 1 and there is no charge flow, as it is expected. On the contrary, with a potential bias $\Delta V = V_L - V_R$ the the fermi functions need to be evaluated to know what direction to expect from the charge current. Since $f_0(x)$ is a monotonically non-increasing function for x, $1 - f_0(x)$ is monotonically increasing for x. Therefore (49) can be addressed by evaluating its variable quantities $\{\mu_d^-, \mu_d^+, V_L, V_R\}$. For a potential bias $\Delta V > 0$ so that $V_L > V_R$ and $\mu_d^{\pm} - eV_R > \mu_d^{\pm} - eV_L$ obtaining $\frac{[1 - f_0(\mu_d^- - eV_L)]}{[1 - f_0(\mu_d^- - eV_R)]} < 1$ and $\frac{f_0(\mu_d^+ - eV_R)}{f_0(\mu_d^+ - eV_L)} < 1$, and we know that the product of two numbers smaller than 1 is still lesser than 1. The opposite result is obtained if the potential bias is reversed $\Delta V < 0$. This means that the mean charge current flows in favour of the potential bias even when it is under the influence of the demon. This has an easy interpretation since the reservoir with higher potential has a greater density of charge carriers available for tunneling to the quantum dot, and the reservoir with lower potential has a greater density of holes available for accepting electrons from the quantum dot. However, this does not mean that a change in the chirality of the system does not vary the current output.

Using equations (21), (47) and (48) one can obtain the net charge current that flows into the left reservoir which is represented in **Figure 7** for a temperature $T = 3\Gamma$ and different values of the capacitive asymmetry $\eta = \frac{C_1 - C_2}{C_1 + C_2}$. The top image with $\eta = 0$ represents the situation where the capacitances of both edge states are equal $C_1 = C_2$ so that $\mu_d^+ = \mu_d^-$ hence the demon protocol has no visible influence. Comparing the graphs of **Figure 7** with negative ($C_1 < C_2$) asymmetry values $\eta = -0.5\,, -0.8$ and the top graph without asymmetry $\eta = 0$ we can see that the presence of the demon is flattening the current flow curves for charge moving in the direction $L \to R$ when $\Delta V > 0$ while sharpening the current flow curves for charge moving in the direction $R \to L$ when $\Delta V < 0$. The opposite happens for the graphs with positive ($C_1 > C_2$) asymmetry values $\eta = 0.5\,, 0.8$ where the presence of the demon flattens (sharpens) the current flow curves for $R \to L$ ($L \to R$) when $\Delta V < 0$ ($\Delta V > 0$). This asymmetry of the demon's influence has a direct explanation. Since the demon protocol designates the magnetic field as positive(negative) when the dot is empty (full), the quantum

level of the dot is always $\mu_d^+(\mu_d^-)$ for carriers tunneling into (out of) the dot. But the dot energy level for the first step of the demon protocol is not always higher than the opposite one. Whenever η and ΔV have the same sign, we have $\mu_d^+ > \mu_d^-$, which, instead of inducing current flow opposite to the voltage bias, enhances the flow in favour of it.

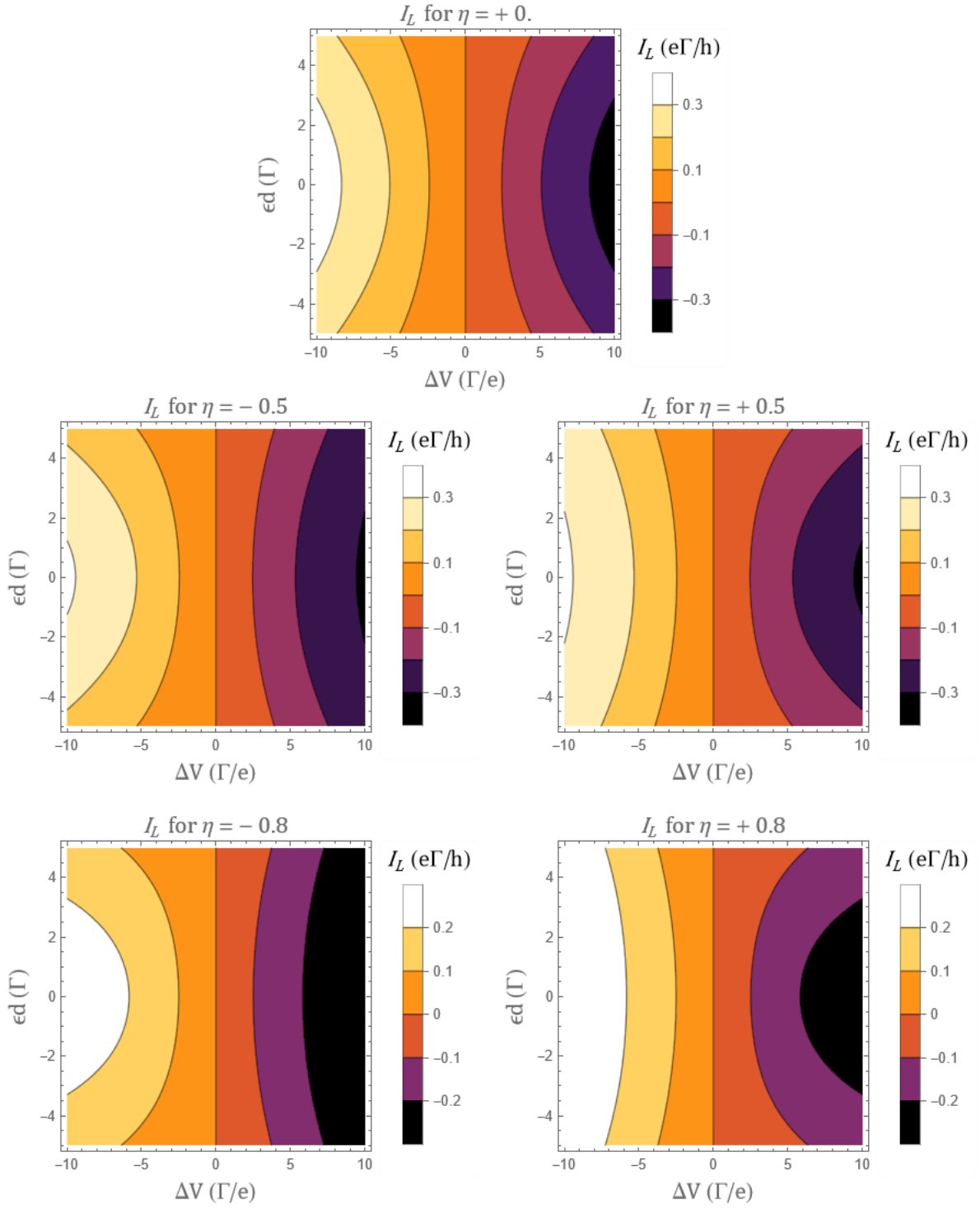

Figure 7: Current flowing into the left reservoir I_L with temperature $T = T_0 = 3\Gamma$ for different values of the capacitance asymmetry η. The result is that current flows out of the left reservoir $(I_L < 0)$ when $\Delta V > 0$ and into the left reservoir $(I_L > 0)$ when $\Delta V < 0$, but the curves of the current intensity are asymmetric for values $\eta \neq 0$

It is also clearly noticeable when comparing the curves of **Figure 7** with the same sign for the capacitive asymmetry $\eta = 0.5$ and $\eta = 0.8$ that the influence of the demon grows with η. This is explained using Information Theory because the information input that enters the demon is proportional to the asymmetry of the electrostatic interaction, which means that the information that the demon can transform into work also grows with η.

4.2. Entropy production

The expression for the entropy production of the system is given in equation (32), which has the same quotient Qu as equation (49), discussed in the previous section. Using this information, we can verify that the second law of thermodynamics is not violated in our setup because the entropy production always verifies that $\dot{S}_i \geq 0$. Both the charge and $\ln Qu$ are positive when $Qu > 1$ and negative when $Qu < 1$ so the product of them is always positive. It can also be confirmed from the graphs in **Figure 8** that the entropy production is positive for the considered range of all the parameters.

We can observe by comparing **Figure 8** and **Figure 7** that the demon influences the symmetry of both the charge current I_L and the entropy production $\dot{S}_i$ which is expected since the information entropy obtained in equation (32) depends on the current intensity. However, we can observe that the demon is producing a larger effect on the entropy when η and ΔV have different signs than where the opposite happens. This asymmetry on the demon's influence on the entropy production comes from the information current that the demon gathers in order to work, which translates into the modification it produces on the system or "*feedback*". When it manages to transport charge carriers in the opposite direction of the potential bias $\mu_d^+ < \mu_d^-$, its feedback is much more significative than when it enhances the current in the direction of the potential bias.

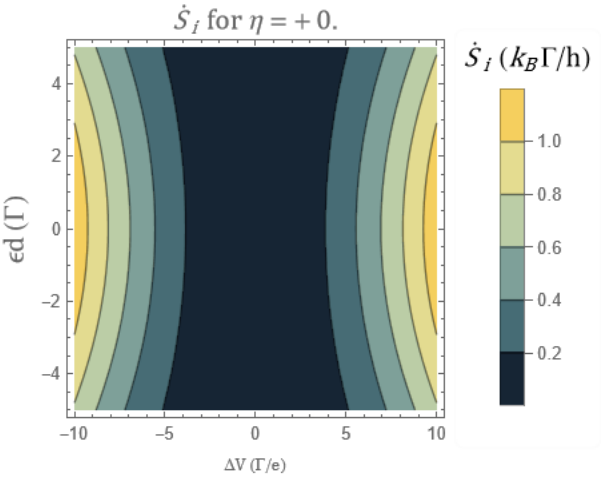

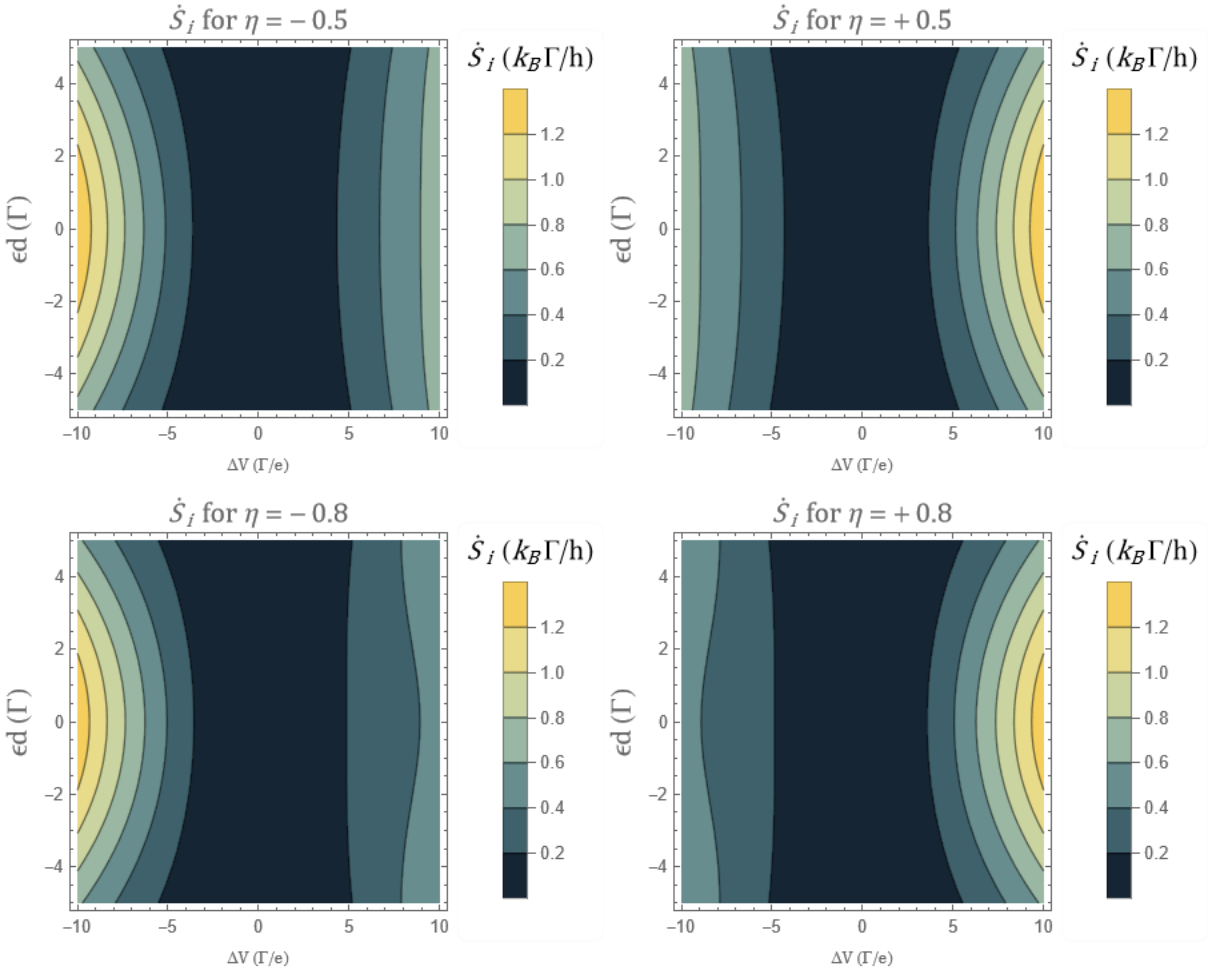

Figure 8: Entropy production $\dot{S}_i$ of the system under the influence of the demon with temperature $T = T_0 = 3\Gamma$ for different values of the capacitance asymmetry η. Entropy production is symmetric for ΔV when the demon has no effect $\eta = 0$. Entropy production is specifically affected when η and ΔV have different signs, in other words, when the demon gives more *"feedback"*.

4.3. Current noise

The noise is the characteristic of the nonequilibrium current that suffers the most drastic change in its symmetry. If we look at **Figure 9** and compare the completely symmetric graph where $\eta = 0$ with any other of the figure it becomes obvious that the effect of the demon has heavily altered the current fluctuations. We can see that the noise remains with similar values under the influence of the demon only when the potential bias and the energy level of the dot are small whereas regions with higher values of these variables have significantly changed. For $\eta < 0$ the noise reaches especially low values for high positive energy levels of the quantum dot ϵ_d and with a very negative voltage bias $\Delta V \ll 0$ so $V_L \ll V_R$ and the current flowing $R \to L$. On the contrary, for $\eta > 0$ the noise reaches these low values for very negative ϵ_d and strong voltage bias $\Delta V \gg 0$ with the current flowing $L \to R$.

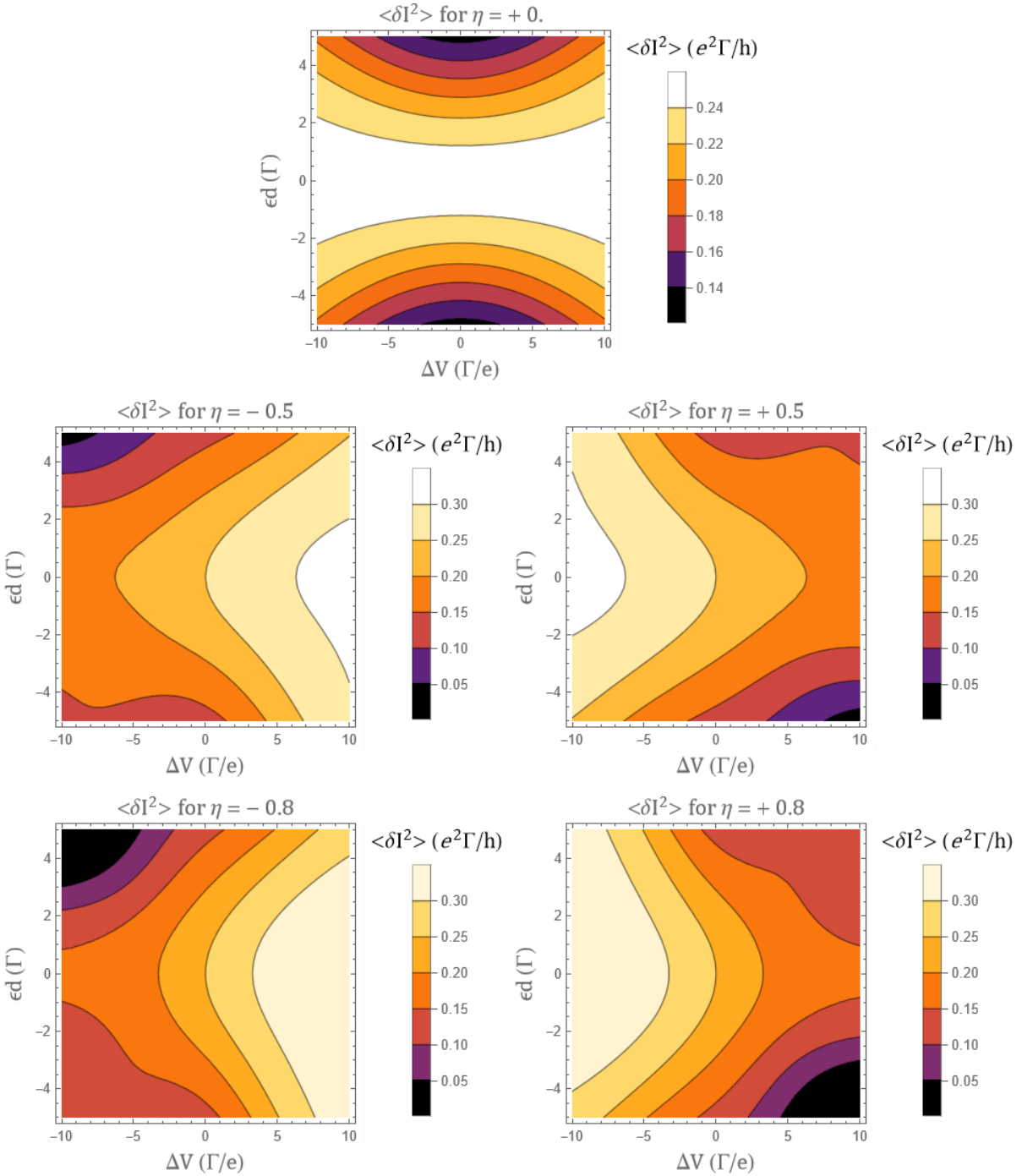

Figure 9: Charge current noise $\langle \delta I^2 \rangle$ with temperature $T = T_0 = 3\Gamma$ for different values of the asymmetry η. If $\eta > 0$, current fluctuations are larger for negative voltage bias $\Delta V < 0$ ($R \rightarrow L$ direction) and if $\eta < 0$, current fluctuations are larger for positive voltage bias $\Delta V > 0$ ($L \rightarrow R$ direction).

4.4. Thermodynamic Uncertainty Relation

All the results obtained above are used in this section for evaluating the Thermodynamic Uncertainty Relation. The original expression of the TUR represented in (1) can be rearranged to become

$$\frac{\langle \delta I^2 \rangle \langle \sigma \rangle}{2\langle I \rangle^2} = \frac{\langle \delta I^2 \rangle \dot{S}_i}{2I_L^2} \geq 1 \qquad (50)$$

Hence, for the TUR to be violated this inequality has to be false. The calculations of the left side of the inequality (50) are represented for the different values of the capacitance asymmetry in **Figure 10** and **Figure 11**. However, before we talk about these results, it is important to point out that the black line in the middle of the graphs is a mathematic singularity caused by the charge current and the entropy production of the system being zero when no potential bias is applied (see **Figure 7** and**Figure 8**) and not a physical outcome.

a)

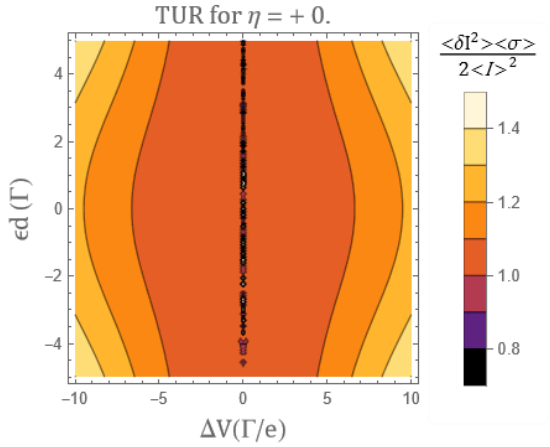

b)

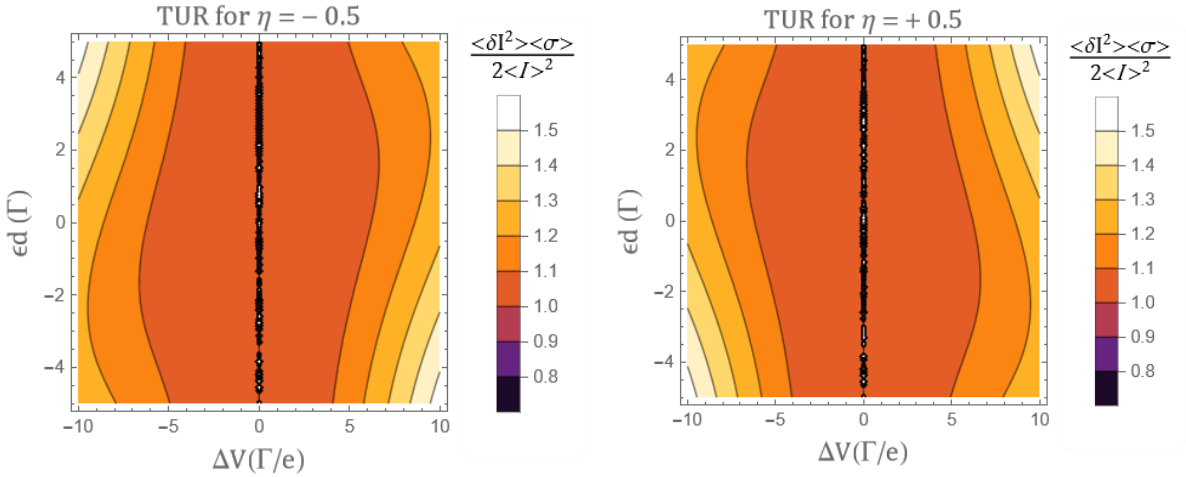

Figure 10: a) Representation of the TUR for temperature $T = T_0 = 3\Gamma$ when there is no capacitance asymmetry $\eta = 0$. b) Representation of the TUR for temperature $T = T_0 = 3\Gamma$ with capacitance asymmetry but no demon protocol.

In **Figure 10 a)** we observe that the system verifies the TUR when there is no capacitance asymmetry, which is an expected outcome since it was already confirmed that for $\eta = 0$ the system is not affected by the demon in a way that time reversal symmetry can be broken. In **Figure 10 b)** we can also see two more graphs where the capacitance asymmetry is $\eta \neq 0$ but the demon protocol is not active. Time

reversal symmetry is not broken here either because, even though there is a capacitive asymmetry that affects the transport properties of the system, the chirality of it does not vary in time and the local detailed balance is not broken.

However, **Figure 11** shows very different results. We can see that the TUR is violated under certain conditions of voltage bias ΔV and energy level ϵ_d of the quantum dot. This is possible because the demon protocol takes advantage of the chirality of the system to break time-reversal symmetry. This also triggers the breaking of the local detailed balance which is a necessary condition for the TUR to apply to Markovian Systems. Thus, we can see in the graphs of **Figure 11** that the thermodynamic uncertainty relation is not satisfied here for quantum dot energy levels around $|\epsilon_d| > 2\Gamma$ because the left side of the Inequality (50) is less than the unit. It can be observed that the voltage bias, the capacitive asymmetry, and the level of the quantum dot are related to the quotient evaluated as follows: When $|\eta|$ grows, less voltage bias ΔV is needed and the value of the energy level of the quantum dot can be lower for the TUR to be violated. The opposite happens when $|\eta|$ decreases.

By comparing two graphs of **Figure 11**, say $\eta = -0.8$ and $\eta = +0.8$ we notice that inverting the scale of the energy level of the dot while inverting the scale of the applied potential bias gives the same result as switching the sign of the capacitive asymmetry, just like it did for the current noise. Therefore, these results can be understood as symmetric. We can also notice how the TUR is violated in both cases: when the potential bias and the capacitive asymmetry have equal signs, which is where $\mu_d^+ < \mu_d^-$ and the noise is smaller and, with less intensity, when the potential bias and the capacitive asymmetry have different signs, which is where more information is gathered and erased by the demon. This can be interpreted

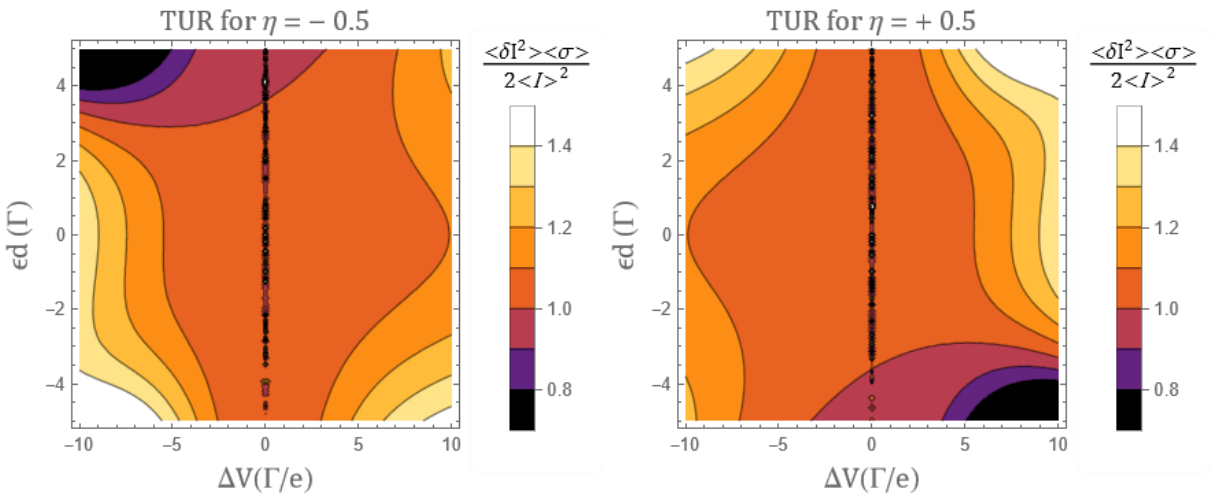

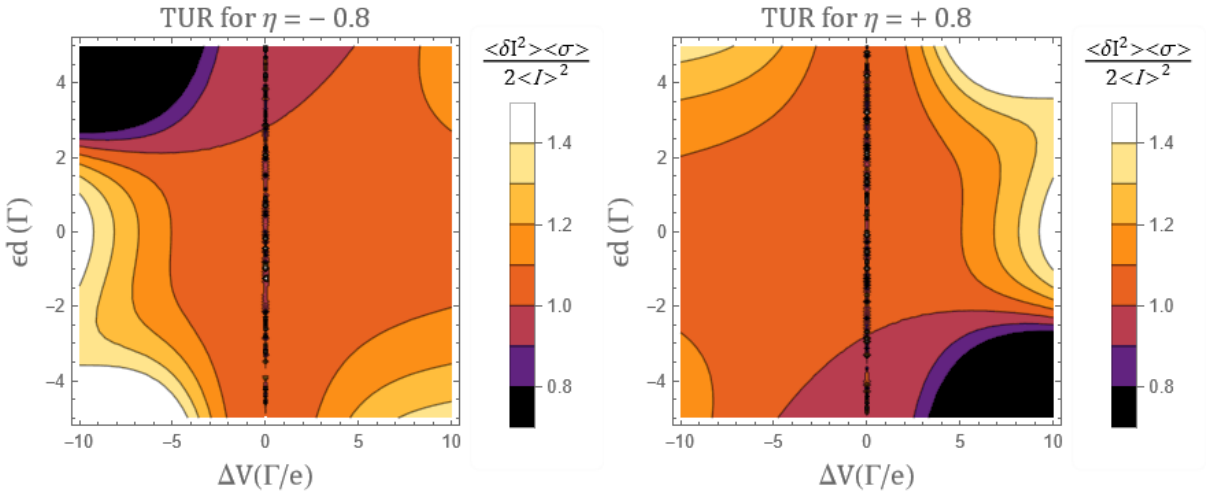

Figure 11: Representation of the TUR quotient at temperature $T = T_0 = 3\Gamma$ with different capacitance asymmetries η when the demon protocol is applied.

6. Conclusions

We have studied how the action of a Maxwell Demon affects the satisfaction of The Thermodynamic Uncertainty Relation for Markovian systems. Taking advantage of the chirality of a topological system, the demon can break the symmetry of the electrochemical potential and the transition rates of the states by switching the magnetic field. We observed that this only happens if there is asymmetry between the capacitive couplings of the edge states because the demon influences the quantum transport properties only if they are affected by the switch in the magnetic field. Then, we have shown that the Demon's influence has altered the entropy and precision of a nonequilibrium observable generated by a Markovian process in a chiral system in a way that did not satisfy the TUR. This was possible because the implementation of the demon used the Quantum Hall Effect to break the time-reversal symmetry and therefore breaking the local detailed balance. This result was observed to be more significant when the potential bias or the energy levels of the system were greater, reducing even further the current fluctuations and dissipation.

Bibliography

[1] R. Feynman, "There's plenty of room at the bottom," in *Feynman and Computation*, 2018. doi: 10.1201/9780429500459.

[2] L. Xiu, "Time Moore: Exploiting Moore's Law from the Perspective of Time," *IEEE Solid-State Circuits Magazine*, vol. 11, no. 1. 2019. doi: 10.1109/MSSC.2018.2882285.

[3] G. E. Moore, "Cramming more components onto integrated circuits," *Proceedings of the IEEE*, vol. 86, no. 1, 1998, doi: 10.1109/JPROC.1998.658762.

[4] K. von Klitzing, "Quantum hall effect: Discovery and application," *Annual Review of Condensed Matter Physics*, vol. 8. 2017. doi: 10.1146/annurev-conmatphys-031016-025148.

[5] T. R. Gingrich, J. M. Horowitz, N. Perunov, and J. England, “Dissipation bounds all steady-state current fluctuations,” Dec. 2015, doi: 10.1103/PhysRevLett.116.120601.

[6] A. Dechant and S. I. Sasa, “Entropic bounds on currents in Langevin systems,” *Phys Rev E*, vol. 97, no. 6, 2018, doi: 10.1103/PhysRevE.97.062101.

[7] S. Saryal, H. M. Friedman, D. Segal, and B. K. Agarwalla, “Thermodynamic uncertainty relation in thermal transport,” *Phys Rev E*, vol. 100, no. 4, 2019, doi: 10.1103/PhysRevE.100.042101.

[8] Y. Hasegawa, “Quantum Thermodynamic Uncertainty Relation for Continuous Measurement,” *Phys Rev Lett*, vol. 125, no. 5, 2020, doi: 10.1103/PhysRevLett.125.050601.

[9] A. C. Barato and U. Seifert, “Thermodynamic Uncertainty Relation for Biomolecular Processes,” *Phys Rev Lett*, vol. 114, no. 15, Apr. 2015, doi: 10.1103/PhysRevLett.114.158101.

[10] R. Kubo, M. Toda, and N. Hashitsume, *Statistical Physics II: Nonequilibrium Statistical Mechanics*, 2nd ed. Stuttgart: Springer Berlin, Heidelberg, 1991.

[11] R. Kulik and P. Soulier, “Markov chains,” in *Springer Series in Operations Research and Financial Engineering*, 2020. doi: 10.1007/978-1-0716-0737-4_14.

[12] J. M. Horowitz and T. R. Gingrich, “Proof of the finite-time thermodynamic uncertainty relation for steady-state currents,” *Phys Rev E*, vol. 96, no. 2, 2017, doi: 10.1103/PhysRevE.96.020103.

[13] M. Polettini, A. Lazarescu, and M. Esposito, “Tightening the uncertainty principle for stochastic currents,” *Phys Rev E*, vol. 94, no. 5, 2016, doi: 10.1103/PhysRevE.94.052104.

[14] T. Ihn, *Semiconductor Nanostructures: Quantum States and Electronic Transport*, vol. 9780199534425. 2010. doi: 10.1093/acprof:oso/9780199534425.001.0001.

[15] D. Delagebeaudeuf and N. T. Linh, “Metal– (n) AIGaAs–GaAs Two-Dimensional Electron Gas FET,” *IEEE Trans Electron Devices*, vol. 29, no. 6, 1982, doi: 10.1109/T-ED.1982.20813.

[16] D. K. Ferry, S. M. Goodnick, and J. Bird, *Transport in Nanostructures*. 2009. doi: 10.1017/CBO9780511840463.

[17] M. Fox and R. Ispasoiu, “Quantum wells, superlattices, and band-gap engineering,” in *Springer Handbooks*, 2017. doi: 10.1007/978-3-319-48933-9_40.

[18] Y. K. A. Lau, D. J. Chernak, M. J. Bierman, and S. Jin, “Epitaxial growth of hierarchical PbS nanowires,” *J Mater Chem*, vol. 19, no. 7, 2009, doi: 10.1039/b818187j.

[19] G. Schedelbeck, W. Wegscheider, M. Bichler, and G. Abstreiter, “Coupled quantum dots fabricated by cleaved edge overgrowth: From artificial atoms to molecules,” *Science*, vol. 278, no. 5344. 1997. doi: 10.1126/science.278.5344.1792.

[20] A. Alkhatib and A. Nayfeh, “A complete physical germanium-on-silicon quantum dot self-Assembly process,” *Sci Rep*, vol. 3, 2013, doi: 10.1038/srep02099.

[21] G. R. Rosselló, “DOCTORAL THESIS 2018 HEAT AND CHARGE TRANSPORT IN NANOSTRUCTURES: INTERFERENCE, AC-DRIVING, ENVIRONMENT, AND FEEDBACK.”

[22] “The sorting demon of Maxwell,” *Nature*, vol. 20, no. 501, 1879, doi: 10.1038/020126a0.

[23] M. Esposito and C. van den Broeck, “The Three Faces of the Second Law: I. Master Equation Formulation,” May 2010, doi: 10.1103/PhysRevE.82.011143.

[24] C. E. Shannon, “The Mathematical Theory of Communication,” *M.D. Computing*, vol. 14, no. 4, 1997, doi: 10.2307/410457.

[25] C. W. Gardiner and P. Zoller, *Quantum noise: a handbook of Markovian and non-Markovian quantum stochastic methods with applications to quantum optics*, vol. 16, no. 10. 2004.

[26] C. Flindt, “Electrons in Nanostructures - coherent manipulation and counting statistics,” Technical University of Denmark, Lyngby, 2007.

[27] C. Flindt, T. Novotný, A. Braggio, M. Sassetti, and A. P. Jauho, “Counting statistics of non-Markovian quantum stochastic processes,” *Phys Rev Lett*, vol. 100, no. 15, 2008, doi: 10.1103/PhysRevLett.100.150601.

[28] G. Chen, M. S. Dresselhaus, G. Dresselhaus, J. P. Fleurial, and T. Caillat, “Recent developments in thermoelectric materials,” *International Materials Reviews*, vol. 48, no. 1, 2003, doi: 10.1179/095066003225010182.